PASJ: Publ. Astron. Soc. Japan , 1–??,

Spin-Orbit Alignment of the TrES-4 Transiting Planetary System and Possible Additional Radial Velocity Variation*

Norio Narita,[1,2] Bun'ei Sato,[3] Teruyuki Hirano,[4] Joshua N. Winn,[5]
Wako Aoki,[1] and Motohide Tamura,[1]
[1] *National Astronomical Observatory of Japan, 2-21-1 Osawa, Mitaka, Tokyo, 181-8588, Japan*
[2] *Kavli Institute for Theoretical Physics, UCSB, Santa Barbara, CA 93106-4030, USA*
[3] *Global Edge Institute, Tokyo Institute of Technology, 2-12-1 Ookayama, Meguro, Tokyo, 152-8550, Japan*
[4] *Department of Physics, The University of Tokyo, Tokyo, 113–0033, Japan*
[5] *Department of Physics, and Kavli Institute for Astrophysics and Space Research, Massachusetts Institute of Technology, Cambridge, MA 02139, USA*
norio.narita@nao.ac.jp

(Received 2010 February 4; accepted 2010 March 11)

Abstract

We report new radial velocities of the TrES-4 transiting planetary system, including observations of a full transit, with the High Dispersion Spectrograph of the Subaru 8.2m telescope. Modeling of the Rossiter-McLaughlin effect indicates that TrES-4b has closely aligned orbital and stellar spin axes, with $\lambda = 6.3^\circ \pm 4.7^\circ$. The close spin-orbit alignment angle of TrES-4b seems to argue against a migration history involving planet-planet scattering or Kozai cycles, although there are two nearby faint stars that could be binary companion candidates. Comparison of our out-of-transit data from 4 different runs suggest that the star exhibits radial velocity variability of $\sim$20 m s^{-1} in excess of a single Keplerian orbit. Although the cause of the excess radial velocity variability is unknown, we discuss various possibilities including systematic measurement errors, starspots or other intrinsic motions, and additional companions besides the transiting planet.

Key words: stars: planetary systems: individual (TrES-4) — stars: rotation — stars: binaries: general — techniques: radial velocities — techniques: spectroscopic

1. Introduction

Transiting planets provide us with valuable opportunities to characterize exoplanetary systems. One such opportunity is to measure the Rossiter-McLaughlin effect (hereafter the RM effect: Rossiter 1924, McLaughlin 1924), an apparent radial velocity anomaly during a planetary transit, which is caused by a partial eclipse of the rotating surface of the host star. By measuring and modeling this effect, one can measure the sky-projected angle between the stellar spin axis and the planetary orbital axis. Many theoretical investigations of the RM effect have been presented (e.g., Ohta et al. 2005; Giménez 2006; Gaudi & Winn 2007; Hirano et al. 2010), and observations of the RM effect have been reported for about 20 transiting planetary systems (for the most recent compilation, see Jenkins et al. 2010 and references therein). One of the main theoretical motivations to observe the RM effect is that the observed degree of spin-orbit alignment is thought to be connected with the migration history of the transiting planet.

The most frequently discussed planetary migration mechanisms are (1) gravitational interaction between a protoplanetary disk and a growing planet (disk-planet interaction models, e.g., Lin & Papaloizou 1985; Lin et al. 1996; Ida & Lin 2004), (2) gravitational planet-planet scattering and subsequent tidal evolution (planet-planet scattering models, e.g., Rasio & Ford 1996; Marzari & Weidenschilling 2002; Nagasawa et al. 2008; Chatterjee et al. 2008), or (3) the Kozai mechanism caused by a distant massive companion and subsequent tidal evolution (Kozai migration models, e.g., Wu & Murray 2003; Takeda & Rasio 2005; Fabrycky & Tremaine 2007; Wu et al. 2007). These scenarios are not necessarily mutually exclusive, but to the extent that they are, disk-planet interaction models would predict small orbital eccentricities and good spin-orbit alignments, while planet-planet scattering models and Kozai migration models predict a broader range of eccentricities and spin-orbit alignment angles. Until about a year ago, all of the measurements indicated close alignments, but recently 6 transiting planets have been reported with significant misalignments: XO-3b (Hébrard et al. 2008; Winn et al. 2009b), HD 80606b (Moutou et al. 2009; Pont et al. 2009a; Winn et al. 2009c), WASP-14b (Johnson et al. 2009; Joshi et al. 2009), HAT-P-7b (Narita et al. 2009a; Winn et al. 2009a), CoRoT-1b (Pont et al. 2009b), and WASP-17b (Anderson et al. 2010). With this increase in the number of measurements, and the diversity of results, we are approaching the time when we may test the validity and applicability of the different planetary migration models.

* Based on data collected at Subaru Telescope, which is operated by the National Astronomical Observatory of Japan.

The main target of this paper is TrES-4b, which is a transiting exoplanet discovered by Mandushev et al. (2007) (hereafter M07) in the course of the TrES survey, supplemented by Keck radial velocity measurements. The planet orbits an F8 (Daemgen et al. 2009) host star every 3.55 days and is one of the most "inflated" hot Jupiters with a radius of about 1.8 $R_{\rm Jup}$, which places this planet to be one of the least density exoplanets ever discovered. Refined spectroscopic and photometric characteristics of the host star TrES-4 were presented by Sozzetti et al. (2009) (hereafter S09). The amplitude of the RM effect for TrES-4b was expected to be large, because of the large projected equatorial rotational velocity of the TrES-4 star ($V \sin I_s = 8.5$ km s^{-1}; S09). In addition, Daemgen et al. (2009) have recently reported a possible companion star around the TrES-4 system. Although it has not yet been confirmed that the companion is a true physical binary as opposed to a chance alignment, a companion star would raise the possibility of migration via Kozai cycles, lending additional motivation to the study of the RM effect in this system. We note that we adopt "TrES-4" as the host star name and "TrES-4b" as the planet name in this paper, although the planet was originally named "TrES-4" by the discoverers (see M07). The reason of our choice is because recent papers on this system (e.g., Daemgen et al. 2009, which we referred in this paper) often describe the host star as "TrES-4". Thus we consider that it would be confusing for readers if we describe the planet as "TrES-4" in our paper, and we hope to avoid such confusions.

In this paper, we present new measurements of the radial velocity of TrES-4 made with the Subaru 8.2m telescope. Although TrES-4 is relatively faint ($V = 11.6$), the large aperture of the Subaru telescope has enabled us to measure radial velocities of TrES-4 with high precision. Our radial velocity dataset consists of 23 samples covering a full transit, and 8 samples obtained outside of transits on 3 different nights. In addition to reporting the spin-orbit alignment angle of TrES-4b, we also report the observation of radial velocity variation in excess of the previously observed single Keplerian orbit, and we confirm through direct imaging with the HDS slit viewer that there are candidate companion stars.

The rest of this paper is organized as follows. Section 2 summarizes our Subaru observations, and section 3 describes analysis procedures of the RM effect of TrES-4b. Section 4 presents our main result on the spin-orbit alignment angle of TrES-4b, and section 5 discusses possible causes of the additional radial velocity variation in this system. Finally, section 6 summarizes the findings of this paper.

2. Observations

We observed a full transit of TrES-4b with the High Dispersion Spectrograph (HDS: Noguchi et al. 2002) on the Subaru 8.2m telescope on UT 2007 July 13. In addition, we measured radial velocities on UT 2007 August 5, UT 2008 March 9, and UT 2008 May 30, when transits were not occurring. For all observations, we employed the same setup. We used the standard I2a setup of the HDS, a slit width of $0\farcs8$ corresponding to a spectral resolution of about 45,000, and the iodine gas absorption cell for precise differential radial velocity measurements. The exposure times for the radial velocity measurements were 12–30 minutes, yielding a typical signal-to-noise ratio (SNR) of approximately 80–100 per pixel. We processed the observed frames with standard IRAF[1] procedures and extracted one-dimensional spectra. We note that in about half of the exposures, light from a nearby companion star (see section 3.1) was also admitted through the slit. For this reason, when extracting the spectra we limited the aperture width of echelle orders to 3–4 pixels, to avoid including any significant flux from the companion star. We computed relative radial velocities and uncertainties following the algorithm of Butler et al. (1996) and Sato et al. (2002), as described in Narita et al. (2007). We estimated the internal measurement uncertainty of each radial velocity based on the scatter of radial velocity solutions for ∼4 Å segments of each spectrum. The typical internal uncertainties were 15–20 m s^{-1}, which is worse than typical cases having similar SNR due to relatively rapid rotation of TrES-4. The radial velocities and uncertainties are summarized in Table 1.

3. Analyses

3.1. HDS Slit Viewer Images

The slit viewer of the Subaru HDS has a 512×512 CCD, providing unfiltered 60"×60" field of view images. During the HDS observations, we found two nearby companion stars in HDS slit viewer images. One is the companion star which Daemgen et al. (2009) also reported to the north of TrES-4, and the other is a newly-discovered star located in west-southwest. Figure 1 shows 4 magnified portions of slit viewer images obtained on UT 2007 July 13 (upper left), UT 2007 August 5 (lower left), UT 2008 March 9 (upper right), and UT 2009 July 12 (lower right). North is up and east is left for these images, and the field of view is 20"×20". Our ability to perform astrometry and photometry on these images is limited, since TrES-4 located on the slit. For the north companion star, we roughly estimate the separation angle as $\sim 1\farcs56$ (~ 13 pixels) and the position angle as $\sim 0^\circ$ (almost true north). These findings are consistent with those of Daemgen et al. (2009). While the west-southwest companion star is located at the separation angle of $\sim 7\farcs8$ (~ 65 pixels) and the position angle of $\sim 249^\circ$. We also estimate that the companion stars are at least 4 magnitudes fainter than TrES-4 in visible wavelength. Although neither our data nor the data of Daemgen et al. (2009) can be used to tell whether or not the companion star is physically associated with TrES-4, it may be possible to do so with multiband IR (for example, *JHK* band) photometry with adaptive optics, which

[1] The Image Reduction and Analysis Facility (IRAF) is distributed by the U.S. National Optical Astronomy Observatories, which are operated by the Association of Universities for Research in Astronomy, Inc., under cooperative agreement with the National Science Foundation.

would be very useful to study common proper motion, color-magnitude relation, and spectral type of the companion stars. Such follow-up observations will enable us to investigate the binarity of the companion stars.

3.2. Simulated Formula for the Rossiter-McLaughlin Effect

We modeled the RM effect of TrES-4 following the procedure of Winn et al. (2005), as adapted for HDS by Narita et al. (2009a, 2009b) and discussed further by Hirano et al. (2010). We first created a synthetic template spectrum which matches the stellar properties of TrES-4 described by S09, using a model by Coelho et al. (2005). To simulate the disk-integrated spectrum of TrES-4, we applied a rotational broadening kernel of $V \sin I_s = 8.5$ km s^{-1} (S09) and adopted the quadratic limb-darkening parameters for the spectroscopic band as $u_1 = 0.46$ and $u_2 = 0.31$ based on the tables of Claret (2004). To simulate in-transit spectra of TrES-4, we subtracted a scaled-down and velocity-shifted copy of the original unbroadened spectrum, which represents the hidden part of the stellar surface. We created a collection of such simulated spectra for various values of the scaling factor f and the velocity-shift v_p, and computed the apparent radial velocity Δv for each spectrum. We fitted Δv in (f, v_p) space and determined an empirical formula of the RM effect for TrES-4 as

$$\Delta v = -f v_p \left[1.623 - 0.885 \left(\frac{v_p}{V \sin I_s} \right)^2 \right]. \quad (1)$$

3.3. Radial Velocity Modeling

Since we did not have good transit light curves for TrES-4b, we fixed stellar and planetary parameters of TrES-4 to the values reported by S09 as follows; the stellar mass $M_s = 1.404$ $[M_\odot]$, the stellar radius $R_s = 1.846$ $[R_\odot]$, the radius ratio $R_p/R_s = 0.09921$, the orbital inclination $i = 82.59°$, and the semi-major axis in units of the stellar radius $a/R_s = 5.94$. As reported in Narita et al. (2009a, 2009b), these assumptions might lead a certain level of systematic errors in results due to uncertainties in the fixed parameters, especially in i and a/R_s. We estimated such systematic errors in section 4. We also fixed the transit ephemeris $T_c = 2454230.9053$ [HJD] and the orbital period $P = 3.553945$ days based on S09. Although this ephemeris had an uncertainty of 3 minutes for the observed transit, the uncertainty was well within our time-resolution (exposure time of 12–30 minutes and readout time of 1 minute) and thus negligible. The adopted parameters above are summarized in table 2.

Our model had 3 free parameters describing the TrES-4 system: the radial velocity semiamplitude (K), the sky-projected stellar rotational velocity ($V \sin I_s$), and the sky-projected angle between the stellar spin axis and the planetary orbital axis (λ). We also added two offset velocity parameters for respective radial velocity datasets (v_1: our Subaru dataset, v_2: Keck in M07). Note that we fixed the eccentricity (e) to zero at first, and the argument of periastron (ω) was not considered. The assumption of zero eccentricity is reasonable since Knutson et al. (2009) constrained $e \cos\omega < 0.0058$ (3σ) based on Spitzer observations of the secondary eclipse.

We then calculated the χ^2 statistic

$$\chi^2 = \sum_i \left[\frac{v_{i,\mathrm{obs}} - v_{i,\mathrm{calc}}}{\sigma_i} \right]^2, \quad (2)$$

where $v_{i,\mathrm{obs}}$ were the observed radial velocity data and $v_{i,\mathrm{calc}}$ were the values calculated based on a Keplerian motion and on the RM formula given above. σ_i were calculated by the quadrature sum of the internal errors of the observed radial velocities and expected stellar jitter level of 4.4 m s^{-1}. We note that we used the mean value of the case of $\Delta M_V < 1, \Delta F_{\mathrm{CaII}} < 0.6, B-V < 0.6$ in Wright (2005) for the jitter, based on the stellar properties reported by S09. We determined optimal orbital parameters by minimizing the χ^2 statistic using the AMOEBA algorithm (Press et al. 1992). We estimated 1σ uncertainty of each free parameter based on the criterion $\Delta\chi^2 = 1.0$.

4. Results

We first fitted all Subaru radial velocity samples with the published 4 radial velocities presented in M07. The upper panels of figure 2 show the radial velocities as a function of orbital phase plotted with the best-fit model curve, and the lower panels plot the radial velocities as a function of HJD. Best-fit parameter values, uncertainties, and the reduced χ^2 for this fit are summarized in the left column of table 3. The fit is poor, with $\chi^2 = 47.4$ and 30 degrees of freedom ($\chi^2_\nu = 1.58$). Apparently there is an inconsistency between the Subaru out-of-transit velocities, and the M07 Keck velocities, even after allowing for a constant offset between these data sets. Comparison of all the observations suggests that there are additional out-of-transit radial velocity variations of about 20 m s^{-1}, which is the root-mean-squared (rms) residual of the Subaru and Keck data. Although the reason for this excess variability is still unclear, some possible reasons are long-term instrumental instabilities, starspots, intrinsic motions of the stellar surface ("stellar jitter"), and the presence of other bodies in the TrES-4 system. We discuss these possibilities in section 5. Here, we concentrate on a reasonable model of the RM effect in spite of the excess variability, to give our best estimate for the sky-projected spin-orbit angle of the transiting planet TrES-4b.

Our approach was to use the Subaru data from the transit night (UT 2007 July 13), along with the Keck data of M07. We chose not to fit the Subaru data obtained on the other 3 nights outside of transits. The left panel of figure 3 plots the data and the best-fit curve (the solid line), and the right panel shows a zoom of the RM effect. The results are summarized in the middle column of table 3. In this case, the fit is good ($\chi^2_\nu = 0.45$) and the best-fit model indicates a good spin-orbit alignment, with $\lambda = 7.3° \pm 4.6°$. The best-fit model also gives $V \sin I_s = 8.3 \pm 1.1$ km s^{-1}, in agreement with the S09

result based on a spectroscopic line analysis. We note that some of the early RM analyses using the analytic formula for the RM effect (e.g., Ohta et al. 2005; Giménez 2006) tended to overestimate the stellar rotational velocity $V \sin I_s$ (e.g., Winn et al. 2005). Recently Hirano et al. (2010) and Collier Cameron et al. (2009) studied the reason for the discrepancy, and Hirano et al. (2010) reported an improved method to address this problem. The agreement between our RM results and the spectroscopic analysis of S09 suggests that the RM calibration process explained above works well. As for the radial velocity semi-amplitude, the fit indicates $K = 94.9 \pm 7.2$ m s^{-1} (the M07 result was $K = 97.4 \pm 7.2$ m s^{-1} for reference).

In addition, we estimated the sensitivity of our results to the choices of the fixed photometric parameters by fitting the radial velocities using other choices for those parameters: (1) $a/R_s = 6.15$, $i = 82.99°$ (corresponding to 1σ lower limit of the impact parameter in S09); (2) $a/R_s = 5.73$, $i = 82.19°$ (corresponding to 1σ upper limit of the impact parameter in S09). Consequently, we found that respective results for λ and $V \sin I_s$ are; (1) $\lambda = 7.2° \pm 4.5°$ and $V \sin I_s = 8.6 \pm 1.1$ km s^{-1}; (2) $\lambda = 7.5° \pm 4.8°$ and $V \sin I_s = 8.0 \pm 1.1$ km s^{-1}. Thus the conclusion of the spin-orbit alignment does not change, and the uncertainties in the photometric parameters have very little effects on our results.

We noticed that the residuals of the Subaru dataset have a small positive gradient with time (see the right middle panel of figure 3). This indicates that the Subaru data alone prefer a slightly smaller value of K than the joint fit of Subaru and Keck data. We therefore fitted the radial velocities of the Subaru UT 2007 July 13 dataset only, for reference. The best-fit model is shown by the dotted lines in figure 3, and derived parameters are summarized in the right column of table 3. The data indicate a smaller radial velocity semiamplitude, but with a larger uncertainty: $K = 64.6 \pm 27.7$ m s^{-1}. This result may be supporting evidence that a true K for the TrES-4b is actually smaller, although it is not very convincing. In this light, it is interesting to point out that TrES-4b was previously known as the lowest density planet ($\rho = 0.202^{+0.038}_{-0.032}$ g cm^{-3}: S09). Recently WASP-17b ($\rho = 0.092^{+0.054}_{-0.032}$ g cm^{-3}: Anderson et al. 2010) and Kepler-7b ($\rho = 0.166^{+0.019}_{-0.020}$ g cm^{-3}: Latham et al. 2010) were reported to have lower densities than TrES-4b, and thus TrES-4b is currently the third lowest density planet discovered so far. The observed out-of-transit radial velocity variation and the radial velocity gradient around the transit phase may suggest a lower density of TrES-4b than previously reported. Thus it is important to obtain radial velocities of TrES-4 not only to confirm the additional radial velocity variation, but also to measure the density of TrES-4b more precisely. We note that this fit gives a small reduced chi-squared ($\chi^2_\nu = 0.35$) and $\lambda = 5.3° \pm 4.7°$, indicating a good spin-orbit alignment as before.

We adopt a compromise value of the latter 2 models as our representative result, namely $\lambda = 6.3° \pm 4.7°$. The small difference between the results of the latter 2 models shows that there is a small systematic uncertainty due to the choice of model. Consequently, we conclude that the TrES-4b has a small value of λ, based on the model of the RM effect. However, since we could not find a satisfactory solution that explains the all observed radial velocities (including all of the Subaru data and the M07 data), further radial velocity measurements are desired to understand any excess variability and to give greater confidence to the orbital solution.

5. Discussion

5.1. Possible Causes of the Additional Radial Velocity Variation

Since we could not find an appropriate model for the all observed radial velocities at this point (see figure 2), we here discuss possibilities of systematic effects as well as real sources of excess radial velocity variation.

– Instrumental Instability of the Subaru HDS

Since the Subaru radial velocities were gathered on a few days in clusters spanning about 1 year, it is of utmost importance to know the instrumental stability of the HDS. For observations within a single night, Narita et al. (2007) studied the radial velocity standard star HD 185144 and found that the Subaru HDS is stable within a few m s^{-1}. In addition, Winn et al. (2009a) reported that the Subaru HDS is stable within a few m s^{-1} over two weeks based on HAT-P-7 observations. Likewise, Johnson et al. (2008) did not find systematic offsets for the HAT-P-1 system over approximately 1 month, using the same setup (and even some of the same nights) as the TrES-4 observations presented here. However, specific stability over 1 year has not yet been confirmed through monitoring of radial velocity standard stars, although studies for such long-term stability of the Subaru HDS are in progress. Thus we note that the instrumental instability of the Subaru HDS is one of the prime possibilities of a cause of the additional radial velocity variation at this point.

– Starspots

One possibility involves starspots on the photosphere of TrES-4. Since the rotational velocity of TrES-4 is relatively fast ($V \sin I_s = 8.5$ km s^{-1}: S09), stellar spots of similar size to a planet would cause an apparent radial velocity shift like the RM effect, on a timescale of the stellar rotation period ($P_{\rm rot} \approx 11$ days, assuming $\sin I_s \approx 1$). For example, a dark spot of approximately the same size as the planet would lead to a maximum shift of 85 m s^{-1}, while smaller spots with less contrast would contribute smaller velocities. If this is the case, all the RV data are affected. However, one would not expect a hot F8 star to have large spots. It is because M07 did not report such possibility of stellar spots from the TrES transit survey, S09 reported no active Ca HK line emission ($\log R'_{\rm HK} = -5.11 \pm 0.15$), and Knutson et al. (2009) concluded that spot activity is unlikely (but not impossible) based on Spitzer observations. Thus the spot explanation is doubtful, although further long-term photometric monitoring would be useful

to constrain this hypothesis still further.

– *Other Sources of Stellar Jitter*

Another possible explanation of the systematic radial velocity variation is an intrinsic stellar jitter (see e.g., Wright 2005), i.e., motions of the stellar photosphere due to pulsations or other flows. Although an empirical relation reported by Wright (2005) predicted a typical stellar jitter of 4.4 m s^{-1} for stars like TrES-4, it is conceivable that TrES-4 has an unusually unstable photosphere. To explain the observed radial velocities, we would need to invoke a stellar jitter of about 20 m s^{-1} for TrES-4 based on the rms residuals of the Subaru and Keck datasets. The jitter would need to have a time scale longer than a few days, in order to explain why the M07 observations (conducted on consecutive three nights) do not exhibit such a large scatter. In this light the hypothesis that the stellar jitter explains all the excess variability seems too contrived.

– *Contamination of Companion Star's Lights or Sky Backgrounds*

As described by Butler et al. (1996), a slight change in the instrumental profile would result in a systematic shift of the apparent radial velocity. Thus, any contaminating light from the nearby candidate companion star of TrES-4 or sky backgrounds (e.g., moonlight or twilight) may have affected the radial velocities. We limited the aperture width of echelle orders in order to avoid contamination of lights from the north companion star. Moonlight contamination is unlikely since our TrES-4 observations were conducted in clear and moonless time, and sky background levels were still low although 2 exposures (HJD of 2454317.74338 and 2454535.14401) were conducted during twilight. Note that M07 did not report the existence of the companion star, and therefore it is possible that the companion star might have been on the slit during the M07 observations. Such an effect might have caused some systematic shifts in the M07 data. Although we were not able to estimate the systematic effect in the M07 data, it could be a small effect since the companion is very faint.

– *Eccentricity of TrES-4b*

As M07 reported only 4 radial velocity samples, they did not include the eccentricity e and the argument of periastron ω in their radial velocity model. Instead they assumed the orbit to be circular as we have done, and more recently Knutson et al. (2009) found $e\cos\omega < 0.0058$ (3σ) based on Spitzer secondary eclipse observations. With the Subaru data we now have a sufficient number of radial velocity samples to allow the eccentricity and argument of pericenter to be free parameters. However, allowing e and ω to vary does not improve the model fit, and the eccentricity of the best-fit model is nearly zero. This is consistent with the constraint by Knutson et al. (2009). Thus a large eccentricity of TrES-4b could not be the explanation for the observed excess RV variability.

– *Additional Planets*

If the preceding explanations for the observed radial velocity variation could be ruled out, we would consider a possibility of presence of additional planets. This is the most interesting case, however, at this point our Subaru observations were too sparse to find and confirm another periodicity in the radial velocities. We can only conclude that the radial velocity semiamplitude of about 20 m s^{-1} over a year is possible for hypothetical planets in the TrES-4 system. Obviously, further continuous radial velocity monitoring would be necessary to check on this possibility.

6. Summary

We observed radial velocities of TrES-4 including a full transit of TrES-4b with the HDS of the Subaru 8.2m telescope. Our radial velocity modeling has revealed that TrES-4b has a close alignment between the projected orbital and stellar spin axes, based on the RM effect. On the other hand, we could not find a satisfactory Keplerian model that agrees with all the data. Although the true cause of the excess radial velocity variation is still unclear, systematic errors in long-term Subaru observations, stellar spots, a large stellar jitter, or additional planets might play a role in the observed radial velocities. The small spin-orbit alignment angle as well as the small eccentricity of TrES-4b seems to match migration models considering disk-planet interactions rather than planet-planet scattering models or Kozai migration models. Although TrES-4 has the binary candidates to the north and the west-southwest, we did not find supporting evidence of the Kozai migration. To confirm and discriminate the true cause of the radial velocity variation of TrES-4, further radial velocity monitoring and photometric monitoring are highly desired.

We acknowledge the invaluable support for our Subaru observations by Akito Tajitsu, a support scientist for the Subaru HDS. We are deeply grateful for David Charbonneau and the TrES collaboration, who kindly informed us the transit ephemeris of TrES-4b in advance of the publication of the M07 paper. We appreciate a careful reading and insightful comments by the anonymous referee. This paper is based on data collected at Subaru Telescope, which is operated by the National Astronomical Observatory of Japan. The data analysis was in part carried out on common use data analysis computer system at the Astronomy Data Center, ADC, of the National Astronomical Observatory of Japan. N.N. is supported by a Japan Society for Promotion of Science (JSPS) Fellowship for Research (PD: 20-8141), and was also supported in part by the National Science Foundation under Grant No. NSF PHY05-51164 (KITP program "The Theory and Observation of Exoplanets" at UCSB). We wish to acknowledge the very significant cultural role and reverence that the summit of Mauna Kea has always had within the indigenous Hawaiian community.

References

Anderson, D. R., et al. 2010, ApJ, 709, 159
Butler, R. P., Marcy, G. W., Williams, E., McCarthy, C., Dosanjh, P., & Vogt, S. S. 1996, PASP, 108, 500
Chatterjee, S., Ford, E. B., Matsumura, S., & Rasio, F. A. 2008, ApJ, 686, 580
Claret, A. 2004, A&A, 428, 1001
Coelho, P., Barbuy, B., Meléndez, J., Schiavon, R. P., & Castilho, B. V. 2005, A&A, 443, 735
Collier Cameron, A., Bruce, V. A., Miller, G. R. M., Triaud, A. H. M. J., & Queloz, D. 2009, ArXiv e-prints
Daemgen, S., Hormuth, F., Brandner, W., Bergfors, C., Janson, M., Hippler, S., & Henning, T. 2009, A&A, 498, 567
Fabrycky, D., & Tremaine, S. 2007, ApJ, 669, 1298
Gaudi, B. S., & Winn, J. N. 2007, ApJ, 655, 550
Giménez, A. 2006, ApJ, 650, 408
Hébrard, G., et al. 2008, A&A, 488, 763
Hirano, T., Suto, Y., Taruya, A., Narita, N., Sato, B., Johnson, J. A., & Winn, J. N. 2010, ApJ, 709, 458
Ida, S., & Lin, D. N. C. 2004, ApJ, 616, 567
Jenkins, J. M., et al. 2010, ArXiv e-prints
Johnson, J. A., Winn, J. N., Albrecht, S., Howard, A. W., Marcy, G. W., & Gazak, J. Z. 2009, PASP, 121, 1104
Johnson, J. A., et al. 2008, ApJ, 686, 649
Joshi, Y. C., et al. 2009, MNRAS, 392, 1532
Knutson, H. A., Charbonneau, D., Burrows, A., O'Donovan, F. T., & Mandushev, G. 2009, ApJ, 691, 866
Latham, D. W., et al. 2010, ArXiv e-prints
Lin, D. N. C., Bodenheimer, P., & Richardson, D. C. 1996, Nature, 380, 606
Lin, D. N. C., & Papaloizou, J. 1985, in Protostars and Planets II, ed. D. C. Black & M. S. Matthews, 981–1072
Mandushev, G., et al. 2007, ApJL, 667, L195 (M07)
Marzari, F., & Weidenschilling, S. J. 2002, Icarus, 156, 570
McLaughlin, D. B. 1924, ApJ, 60, 22
Moutou, C., et al. 2009, A&A, 498, L5
Nagasawa, M., Ida, S., & Bessho, T. 2008, ApJ, 678, 498
Narita, N., Sato, B., Hirano, T., & Tamura, M. 2009a, PASJ, 61, L35
Narita, N., et al. 2007, PASJ, 59, 763
Narita, N., et al. 2009b, PASJ, 61, 991
Noguchi, K., et al. 2002, PASJ, 54, 855
Ohta, Y., Taruya, A., & Suto, Y. 2005, ApJ, 622, 1118
Pont, F., et al. 2009a, A&A, 502, 695
Pont, F., et al. 2009b, MNRAS, L360+
Press, W. H., Teukolsky, S. A., Vetterling, W. T., & Flannery, B. P. 1992, Numerical recipes in C. The art of scientific computing (Cambridge: University Press, —c1992, 2nd ed.)
Rasio, F. A., & Ford, E. B. 1996, Science, 274, 954
Rossiter, R. A. 1924, ApJ, 60, 15
Sato, B., Kambe, E., Takeda, Y., Izumiura, H., & Ando, H. 2002, PASJ, 54, 873
Sozzetti, A., et al. 2009, ApJ, 691, 1145 (S09)
Takeda, G., & Rasio, F. A. 2005, ApJ, 627, 1001
Winn, J. N., Johnson, J. A., Albrecht, S., Howard, A. W., Marcy, G. W., Crossfield, I. J., & Holman, M. J. 2009a, ApJL, 703, L99
Winn, J. N., et al. 2005, ApJ, 631, 1215
Winn, J. N., et al. 2009b, ApJ, 700, 302
Winn, J. N., et al. 2009c, ApJ, 703, 2091
Wright, J. T. 2005, PASP, 117, 657
Wu, Y., & Murray, N. 2003, ApJ, 589, 605
Wu, Y., Murray, N. W., & Ramsahai, J. M. 2007, ApJ, 670, 820

Table 1. Radial velocities obtained with the Subaru/HDS.

Time [HJD]	Value [m s^{-1}]	Error [m s^{-1}]
2454294.7715	-5.1	18.6
2454294.7901	-12.7	16.2
2454294.7991	-7.3	16.7
2454294.8081	4.5	15.8
2454294.8171	44.1	16.3
2454294.8261	22.5	17.8
2454294.8351	20.7	15.4
2454294.8441	26.8	16.1
2454294.8531	-0.2	16.6
2454294.8621	-10.2	13.7
2454294.8711	-20.9	14.6
2454294.8801	-39.3	13.8
2454294.8891	-52.5	12.8
2454294.8981	-51.6	14.5
2454294.9071	-45.5	15.2
2454294.9161	-77.1	14.6
2454294.9252	-70.0	12.2
2454294.9342	-43.9	13.0
2454294.9432	-41.3	11.9
2454294.9522	-16.5	14.0
2454295.0289	-31.6	14.2
2454295.0379	-36.5	13.1
2454295.0559	-33.5	13.6
2454317.7434	-38.4	15.8
2454317.9553	12.6	19.6
2454535.1010	-10.9	19.3
2454535.1225	-28.2	17.3
2454535.1440	-18.4	18.0
2454616.8015	3.0	18.8
2454616.8162	-24.2	19.6
2454616.8309	-16.4	20.3

Table 2. Adopted stellar and planetary parameters.

Parameter	Value	Source
M_s [$M_\odot$]	1.404	S09
R_s [$R_\odot$]	1.846	S09
R_p/R_s	0.09921	S09
i [°]	82.59	S09
a/R_s	5.94	S09
u_1	0.46	Claret (2004)
u_2	0.31	Claret (2004)
jitter [m s^{-1}]	4.4	Wright (2005)
T_c [HJD]	2454230.9053	S09
P [days]	3.553945	S09

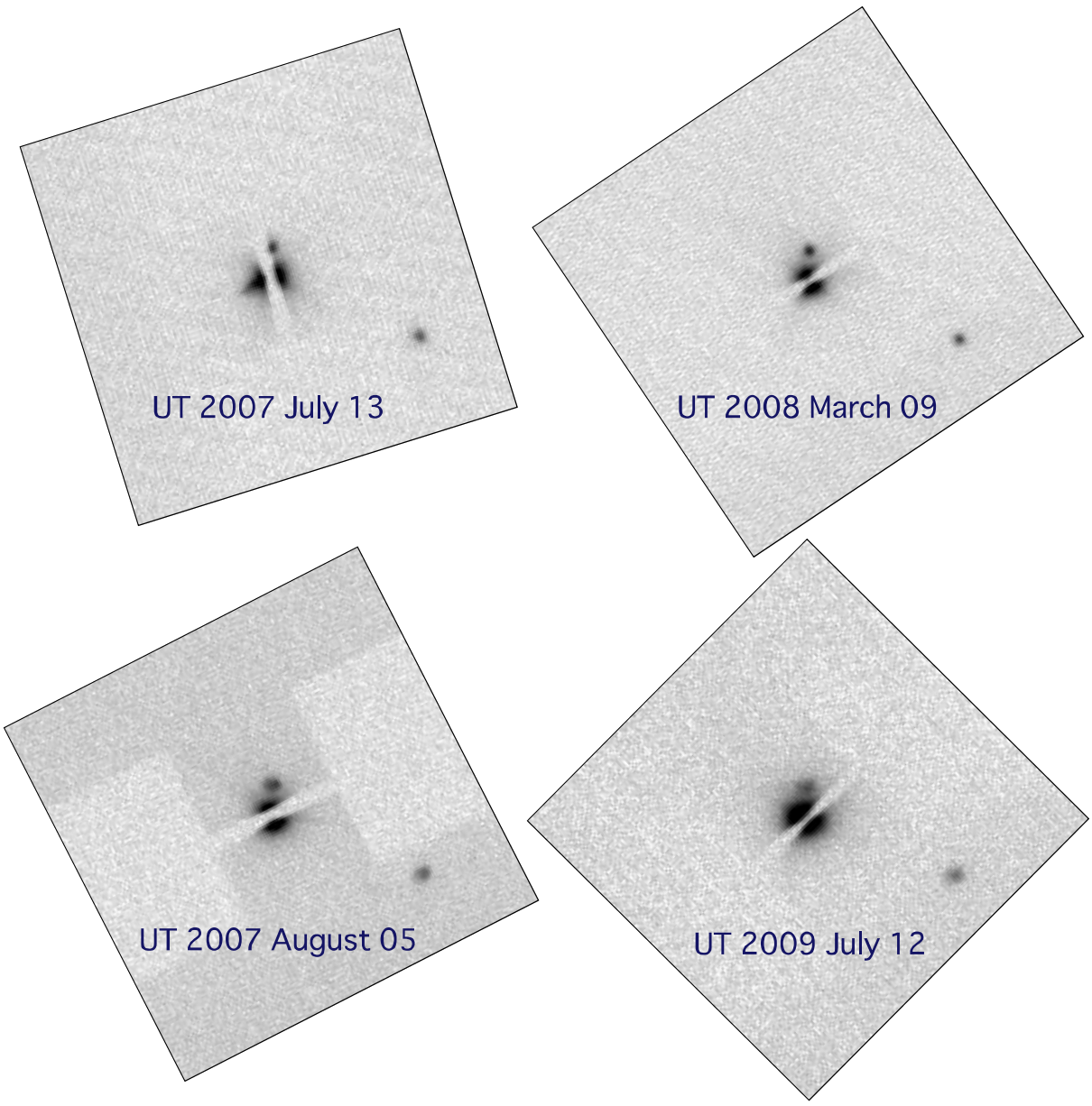

Fig. 1. HDS slit viewer images of TrES-4 taken on UT 2007 July 13 (upper left), UT 2007 August 05 (lower left), UT 2008 March 9 (upper right), and UT 2009 July 12 (lower right). North is up and east is left, and field of view is 20" × 20" for the all images.

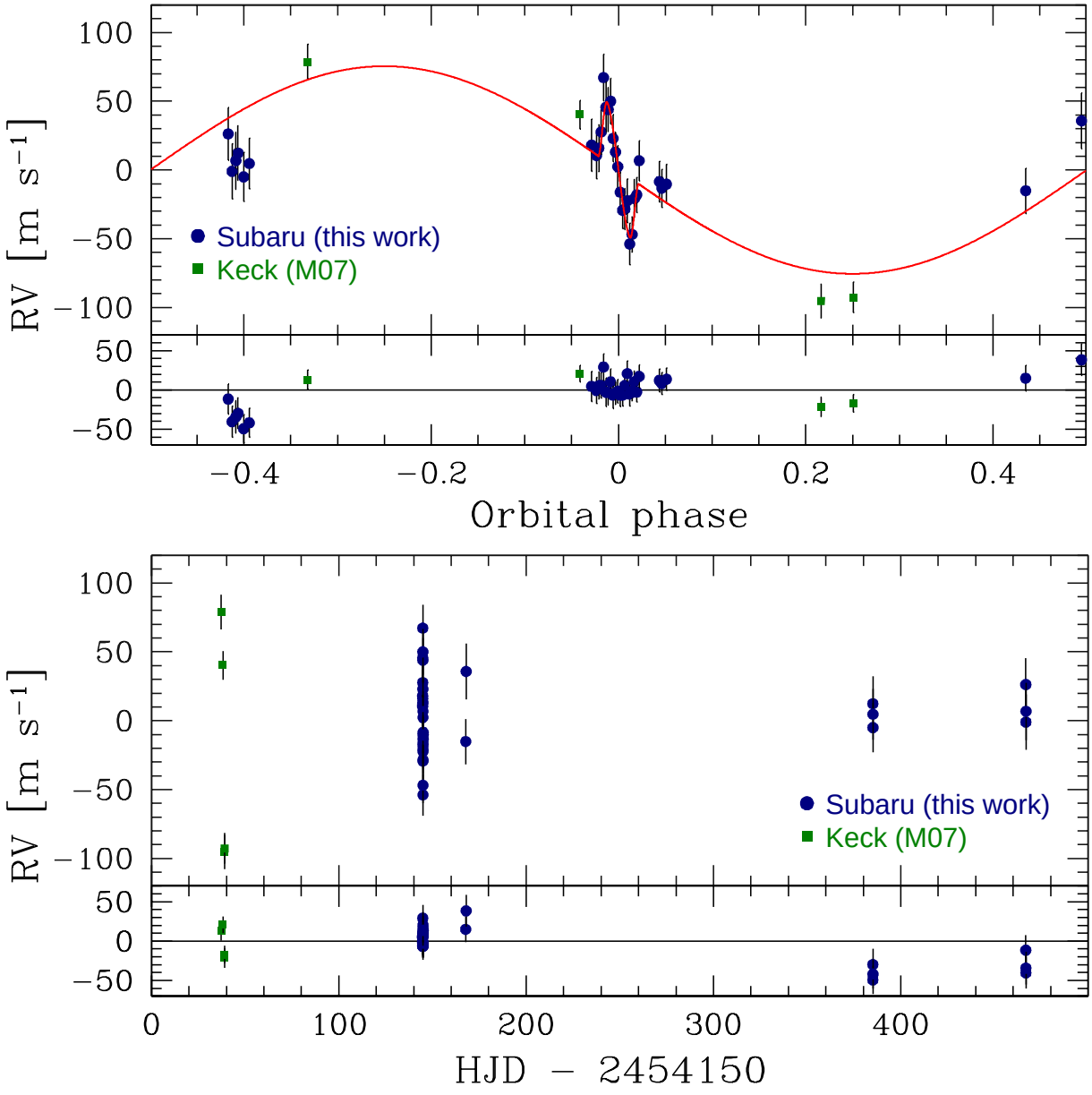

Fig. 2. Radial velocities (RVs) and the best-fit curve of TrES-4 as a function of orbital phase (upper) and as a function of HJD (lower). All Subaru RVs and the M07 RVs are used. Bottom panels: Residuals from the best-fit curve.

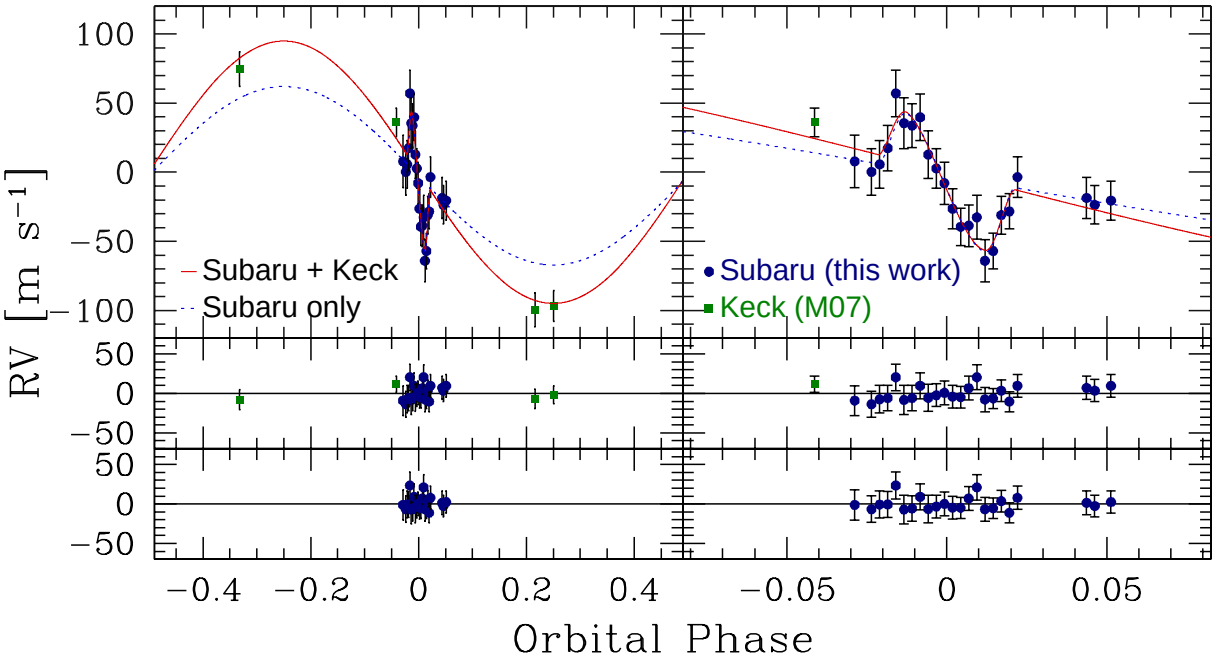

Fig. 3. Top panels: Radial velocities (RVs) and best-fit curves of TrES-4 as a function of orbital phase. The left panels show the entire orbit and the right panels are the zoom of transit phase. The solid line indicates the best-fit curve for the case that Subaru RVs taken on UT 2008 July 13 and the M08 RVs are used, and the dotted line is for the case that only Subaru RVs are used. Middle panels: Residuals from the solid model curve. Bottom panels: Residuals from the dotted model curve.

Table 3. Best-fit values and uncertainties of the free parameters.

	Subaru all + Keck		Subaru transit + Keck		Subaru transit only	
Parameter	Value	Uncertainty	Value	Uncertainty	Value	Uncertainty
K [m s^{-1}]	75.5	±6.3	94.9	±7.2	64.6	±27.7
$V \sin I_s$ [km s^{-1}]	8.3	±1.1	8.3	±1.1	8.7	±1.2
λ [°]	0.0	±4.2	7.3	±4.6	5.3	±4.7
v_1 (Subaru) [m s^{-1}]	-23.2	±3.8	-13.0	±4.6	-15.5	±5.1
rms (Subaru) [m s^{-1}]	19.9	–	9.2	–	8.4	–
v_2 (Keck) [m s^{-1}]	18.7	±5.9	22.9	±6.0	–	–
rms (Keck) [m s^{-1}]	18.4	–	7.9	–	–	–
χ^2/ν	47.36/30	–	9.88/22	–	6.64/19	–